J Appl Electrochem (2008) 38:309–313
DOI 10.1007/s10800-007-9439-5

ORIGINAL PAPER

Effect of temperature on nickel electrodeposition from a nickel sulfamate electrolyte

M. Saitou · S. Oshiro · S. M. Asadul Hossain

Received: 9 May 2007 / Revised: 17 October 2007 / Accepted: 29 October 2007 / Published online: 16 November 2007
© Springer Science+Business Media B.V. 2007

Abstract The effect of temperature on nickel electrodeposition from a nickel sulfamate electrolyte has been investigated. All the experimental points in a plot of nickel film thickness vs. current density collapse onto a single straight line irrespective of deposition temperature. A relation derived from the Butler–Volmer equation is successful in predicting cathode potential shifts caused by change of deposition temperature. Moreover, an interface width, which characterizes the roughness of the surface and is defined by the root mean square of fluctuation in the height, is shown to have a saturated value that is related to the deposition temperature. Thus, two kinds of activation energies for the charge transfer reaction and for grain growth are estimated from the temperature dependence of the cathode potential shift and the grain size.

Keywords Nickel · Electrodeposition · Temperature · Cathode potential shift · Activation energy

1 Introduction

Nickel electrodeposition from nickel sulfamate electrolytes [1] has technological advantages in yielding good physical properties such as low internal stress [2] and in having a current efficiency higher than 98% [3]. Deposition parameters affecting the electrochemical behavior and properties of nickel thin films [4] continue to be studied. Deposition temperature influences the electrochemical processes and the physical properties of electrodeposits from nickel sulfamate electrolytes. For instance, preferential crystallographic growth directions are reported [5] to be significantly influenced by temperature. However, few studies on the effect of temperature on the growth processes in nickel sulfamate electrolytes have been made [3].

An interface width, $w(t)$ [6] defined by Eq. 1 is often employed to determine surface growth models for deposits

$$w(t) = \left(\frac{1}{N}\sum_{i=1}^{N}(h_i - \bar{h})^2\right)^{1/2}, \quad (1)$$

where t is the deposition time, h_i is the height of the deposit above substrate position i and $\bar{h}$ is the average height of the deposit formed by N points. Equation 1 represents the standard deviation of h_i.

In nickel electrodeposition from nickel sulfamate electrolytes, the dynamic behavior of the interface width has been examined and shown to obey scaling laws that statistically characterize the surface growth models [7–9]. The grain size of thin films electrodeposited from nickel chloride electrolytes [10] is reported to increase with increase in deposition temperature. However, there have been few studies on the quantitative relationship between the interface width and the grain size affected by temperature. The present paper will indicate that the interface width increases with current density and saturates, and that there exists a clear correlation between the saturated interface width and the grain size of the nickel electrodeposit.

This paper aims at showing that (1) the relation derived from the Butler–Volmer equation explains the cathode potential shift caused by change of temperature, (2) the saturated interface width is related to the grain size which obeys an Arrhenius-type equation, and (3) the activation energies for the charge transfer reaction in nickel

M. Saitou (✉) · S. Oshiro · S. M. Asadul Hossain
Department of Mechanical Systems Engineering, University of the Ryukyus, 1 Senbaru Nishihara-cho, Okinawa 903-0215, Japan
e-mail: saitou@tec.u-ryukyu.ac.jp

electrodeposition and for grain growth are estimated from the temperature dependence of the cathode potential shift and the grain size.

2 Experimental set-up

ITO glass plates with the root mean square roughness of 1.2 nm and carbon plates were prepared for cathode and anode electrodes. Both electrodes of 10×30 mm^2 were cleaned by a wet process and located parallel in a quiescent bath containing (g l^{-1}): nickel sulfamate, 600; nickel chloride, 5; and boric acid, 40. The bath at pH 4 was held at a temperature from 295 to 323 K. Here to avoid decomposition of nickel sulfamate, an upper temperature of 323 K was chosen. Current density in the range 1–64 mA cm^{-2} was applied. The cathode potential was measured with a Luggin capillary comprising Ag/AgCl electrodes in a KCl solution.

The surface morphologies of the nickel electrodeposits were observed with Confocal Laser Scanning Microscopy (Keyence VF7500) that has a resolution of 0.01 μm in height. The interface width in Eq. 1 was calculated from the surface profile comprising 512 pixels.

To observe grain boundaries of the nickel electrodeposits with Confocal Laser Scanning Microscopy, an electrochemical etching technique was performed. The ITO glass plate on which nickel had been deposited and the carbon plate were located in a 5.4 vol.% sulfuric acid solution. The nickel electrodeposit was slightly etched for 20 s in the solution at a fixed voltage of 2.2 V and at 295 K.

3 Results and discussion

3.1 Nickel film thickness and deposition temperature

Figure 1 shows the dependence of the nickel film thickness on current density at a deposition time of 300 s. It can be seen that all the experimental data lie on the single straight line irrespective of deposition temperature. Additionally, Faraday's law holds true for the electrodeposits of which the current efficiency is 96% for the three different temperatures.

This result leads to a relationship between the cathode potential and deposition temperature as follows. The nickel film thickness is linearly proportional to current density in Fig. 1. Hence, a change of the current density, Δj, caused by a change of deposition temperature ΔT should become zero. If not so, the film thickness varies with change in deposition temperature. In fact the film thickness at 10 mA cm^{-2} for 307 K and that for 317 K have the same value as shown in Fig. 1. The current density is expressed by the Butler–Volmer equation [11]

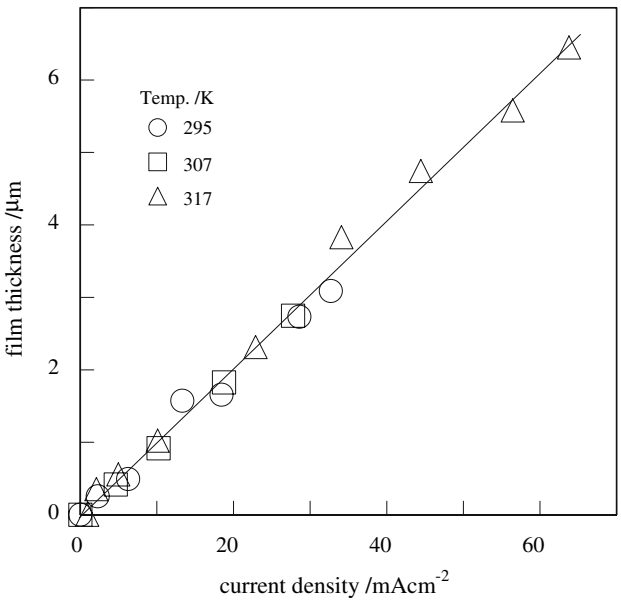

Fig. 1 Plot of film thickness vs. current density for deposition temperature of 295, 307 and 317 K at a deposition time of 300 s

$$j = j_0\left[\exp\left(\frac{zF\alpha_c\eta}{RT}\right) - \exp\left(-\frac{zF(1-\alpha_c)\eta}{RT}\right)\right], \tag{2}$$

where j_0 is the exchange current density which has the form

$$j_0 = \frac{zFk_BT}{h'}\exp\left(-\frac{\Delta G}{RT}\right), \tag{3}$$

where z is the valence number, F is the Faraday constant, α_c is the charge transfer coefficient for the cathodic process, η is the cathode potential, R is the gas constant, k_B is the Boltzmann constant, $h' = h/2\pi$ where h is the Plank constant, ΔG is the free energy change (activation energy) for the charge transfer reaction in nickel electrodeposition, and T is the absolute temperature. For $zF\alpha_c\eta/RT >> 1$, Eq. 2 becomes $j = j_0\exp(zF\alpha_c\eta/RT)$. In this study, it will be shown in Figs. 2, 3 that the cathode potential η becomes greater than 250 mV, which satisfies the condition $zF\alpha_c\eta/RT >> 1$ for $\alpha_c = 0.5$. Combination of Eq. 3 and j for $zF\alpha_c\eta/RT >> 1$ gives the change in current density Δj caused by change of deposition temperature ΔT,

$$\frac{\Delta j}{\frac{zFk_B}{h'}} = (T+\Delta T)\exp\left[\frac{zF\alpha_c(\eta+\Delta\eta)-\Delta G}{R(T+\Delta T)}\right] - T\exp\left[\frac{zF\alpha_c\eta-\Delta G}{RT}\right] = 0. \tag{4}$$

Equation 4 can be rewritten as

$$1 + \frac{zF\alpha_c\Delta\eta}{R\Delta T} - \frac{zF\alpha_c\eta}{RT} + \frac{\Delta G}{RT} = 0, \tag{5}$$

where $\Delta\eta$ is the change of the cathode potential caused by change in temperature ΔT. The solution of the ordinary

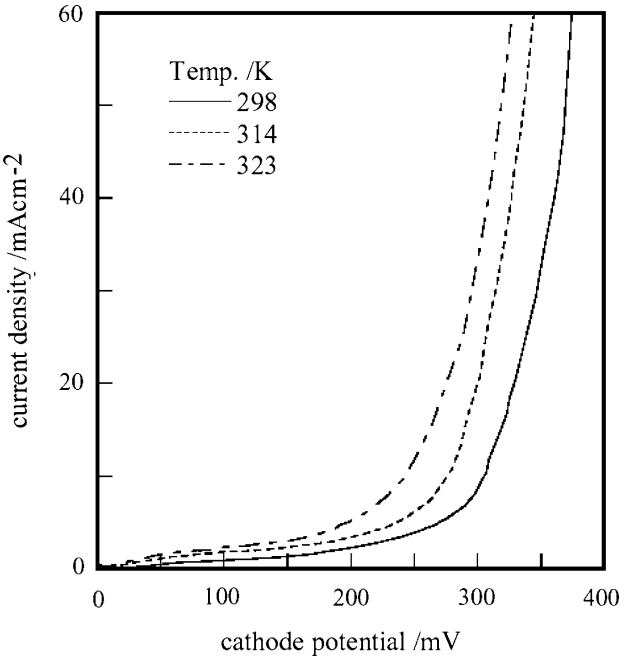

Fig. 2 Typical plot of cathode potential vs. current density for deposition temperatures of 298, 314 and 323 K

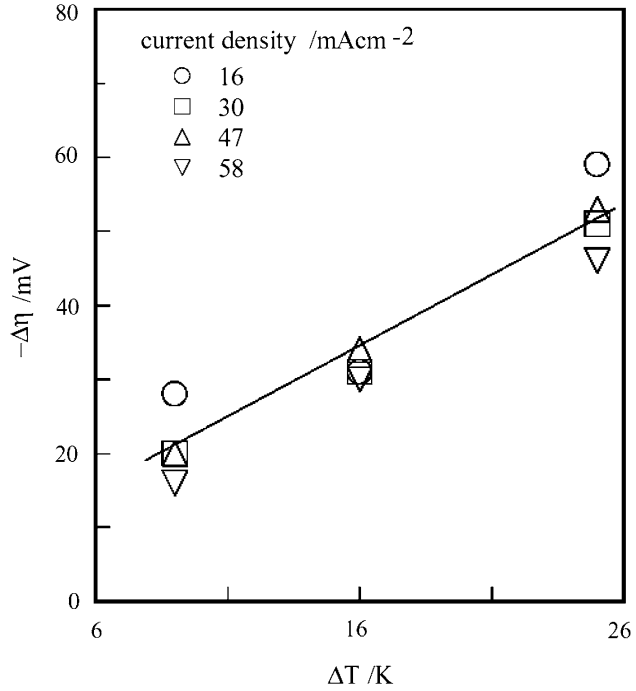

Fig. 3 Plot of cathode potential shift $\Delta\eta$ caused by change in temperature ΔT for different current densities. The values of $\Delta\eta$ and ΔT are obtained from Fig. 2 and the reference temperature T_0 is 298 K

differential equation (5) with two variables T and η is given by

$$\Delta\eta = e^{\int_{\Delta T}\frac{dT}{T}}\left\{\int_{\Delta T}\left(-\frac{\Delta G}{zF\alpha_c T}-\frac{R}{zF\alpha_c}\right)e^{-\int_{\Delta T}\frac{dT}{T}}dT\right\}, \qquad (6)$$

where $\Delta T = T - T_0$ and T_0 is the reference temperature. Finally, the solution becomes

$$\Delta\eta = -\left(\frac{\Delta G}{zF\alpha_c T_0}+\frac{R}{zF\alpha_c}\right)\Delta T. \qquad (7)$$

This equation indicates that the change in cathode potential is linearly proportional to the change in deposition temperature.

Figure 2 shows a plot of the current density vs. the cathode potential for three different temperatures and enables us to estimate the change of cathode potential caused by the change in deposition temperature.

Figure 3 shows the cathode potential shift $\Delta\eta$ caused by change in deposition temperature ΔT for four different current densities using Fig. 2. At a current density greater than 16 mA cm^{-2}, the cathode potential η becomes greater than 250 mV, which satisfies the condition $zF\alpha_c\eta/RT >> 1$ for $\alpha_c = 0.5$. As Eq. 7 predicts, it can be seen from Fig. 3 that the change in cathode potential is linearly proportional to the change in deposition temperature. Thus, the reason why all the experimental points collapse on the single straight line for the different deposition temperature is indicated. The slope best fitted to the data in Fig. 3 gives the activation energy for the charge transfer reaction, $\Delta G = 53.8 \pm 2.3$ kJ mol^{-1}, which is a little larger than that for copper, 50.6 kJ mol^{-1} [12].

3.2 Relation between saturated interface width and grain size

Figure 4a shows a microscope image of nickel grown at 295 K and at a current density of 32.7 mA cm^{-2}, and its surface height measured for the calculation of $w(t)$ in Eq. 1. The surface is smooth and bright with average surface height $\bar{h}$ of 0.21 ± 0.02 μm.

Figure 4b shows the dependence of $w(t)$ on the current density for three different temperatures. The interface width of nickel electrodeposits from the nickel sulfamate electrolyte, $w(t)$ has been reported to have a scaling property with respect to the growth time t [7–9, 13], which is represented by

$$w(t)\sim\begin{cases} t^{\beta}, & t<t_c \\ w_s, & t>t_c \end{cases}, \qquad (8)$$

where t_c is the cross over time, β is called the growth exponent and w_s is the saturated interface width dependent on system size L [6]. The interface width reaches a saturated value w_s at $t = t_c$. In addition, the saturated interface width w_s follows a power law, $w_s \sim L^{\alpha}$. The exponent α is called the roughness exponent. There are contradictory

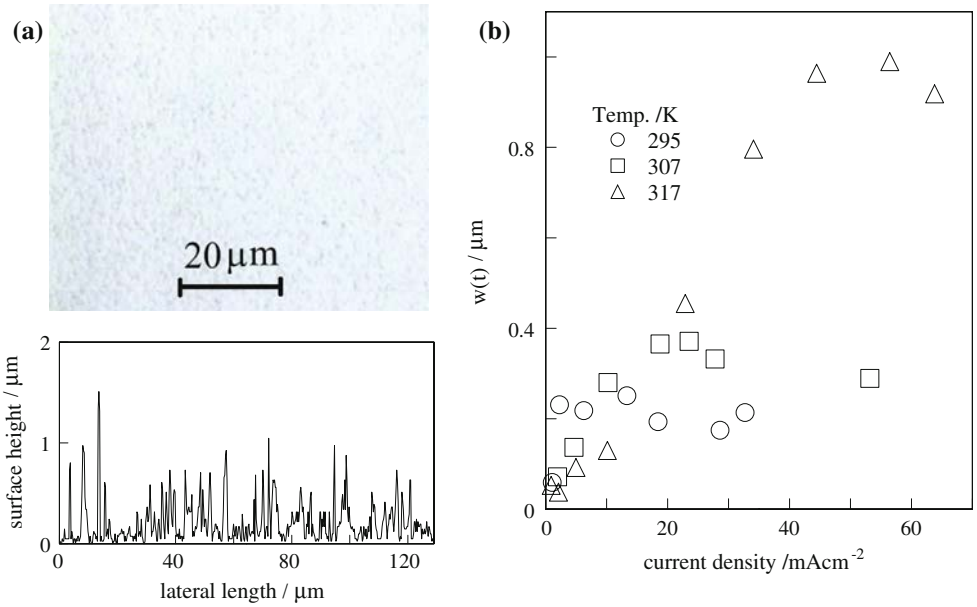

Fig. 4 Surface image, its surface height h_i above a substrate location i and a plot of the interface width in Eq. 1 vs. current density. (**a**) Microscope surface image of the nickel electrodeposit grown for 300 s at 295 K and 32.7 mA cm^{-2}. (**b**) Interface width $w(t)$ saturates with increase in current density

studies on the dependence of the interface width on the current density; references [14, 15] state that the interface width increases at a low current density and decreases at a higher current density and the other reference states [16] vice versa. This is because the interface width used in the References [14–16] may be one at $t < t_c$, that is, the unsaturated interface width.

In fact, in our experiment the unsaturated values of the interface width are observed in Fig. 4b in which all the points are measured at a deposition time of 300 s. For instance, $w(t)$ at less than 40 mA cm^{-2} and at a deposition temperature of 317 K does not reach the saturated interface width w_s. The interface width at less than 40 mA cm^{-2} needs a longer deposition time than 300 s to saturate. At current density greater than 40 mA cm^{-2}, $w(t)$ reaches the saturated value w_s with some scatter. Hence, in this study, w_s is used to investigate a relationship between the saturated interface width and the grain size.

Figure 5 shows a microscope image of the electrodeposit of which the interface width reached the saturated interface width. The surface was slightly etched to observe grain boundaries with Confocal Laser Scanning Microscopy. The grain size was determined by the average of the major and minor axis of the grain in Fig. 5.

The average grain size, $\bar{d}$ and the saturated interface width, w_s for three deposition temperature are plotted in Fig. 6a. The average of $w(t)$ independent of the current density in Fig. 4b is calculated as w_s. For instance, the average of four points at a current density greater than 18 mA cm^{-2} is taken as w_s at a temperature of 307 K. It can be seen that the average grain size increases with an increase in w_s. To determine the activation energy ΔH for grain growth an Arrhenius-type equation is assumed

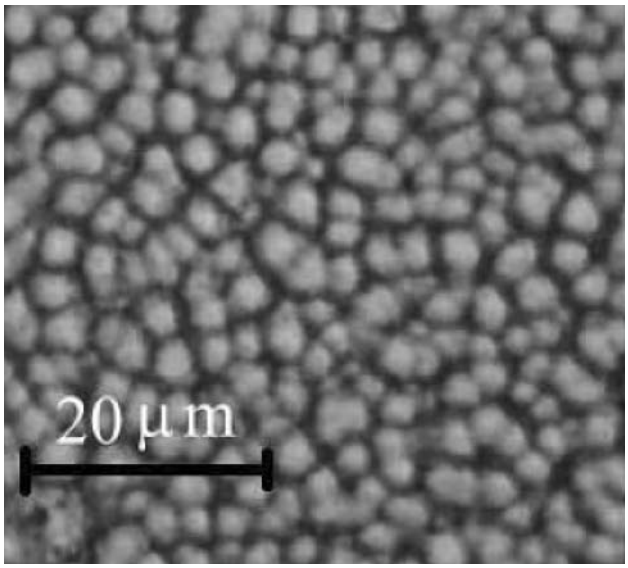

Fig. 5 Typical microscope image of the nickel electrodeposit slightly etched in the 5.4 vol.% sulfuric acid solution at 2.2 V and at 295 K. The nickel electrodeposit was grown for 300 s at 317 K and 63.8 Ma cm^{-2}

$$\bar{d} \propto e^{-\frac{\Delta H}{RT}}, \tag{9}$$

where $\bar{d}$ is the average grain size of the nickel electrodeposits of which the interface width reached the saturated interface width. Figure 6b shows a reciprocal plot of temperature for the average grain size. The slope gives the activation energy for grain growth in the surface, 2.3 ± 0.3 kJ mol^{-1} (0.2 eV per atom), which is approximately equal to the activation energy for self-diffusion on (111) nickel surfaces [17]. However, this may not indicate that the crystallographic surface planes comprise (111).

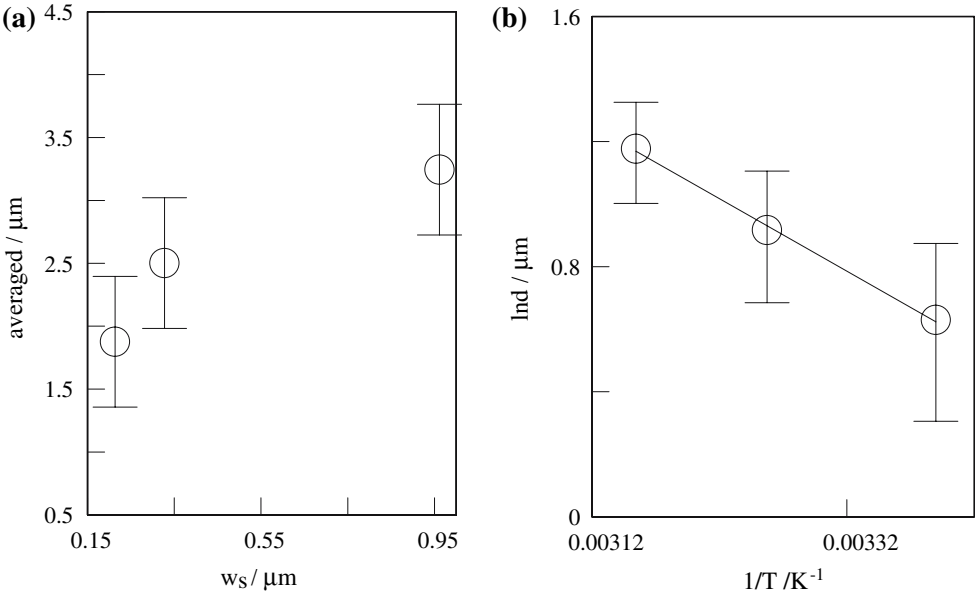

Fig. 6 Relation between saturated interface width and average grain size as a function of temperature. (**a**) Plot of saturated interface width vs. average grain size. (**b**) Arrhenius plot. The activation energy of 2.3 ± 0.3 kJ mol^{-1} is calculated from the slope

Further studies, not only on the crystallographic growth direction [18], but also on the crystallographic surface planes, will be needed.

4 Conclusion

Nickel electrodeposition from nickel sulfamate electrolyte in the temperature range 295–323 K has been investigated. The relation required for all the experimental points in a plot of nickel film thickness vs. current density to collapse to a single straight line is derived. The relation is found to support the experimental result of the cathode potential shift caused by change in temperature. In addition, the interface width $w(t)$ increases with the current density and saturates to a fixed value dependent on deposition temperature. There exists a relation between the saturated interface width and the grain size. Additionally, the activation energies for the charge-transfer reaction and for grain growth are estimated at 53.8 ± 2.3 and 2.3 ± 0.3 kJ mol^{-1}.

References

1. Baudrand D (1996) Met Finishing 94:15
2. Goods SH, Kelly JJ, Talin AA, Michael JR, Watson RM (2006) J Electrochem Soc 153:C325
3. Tsuru Y, Nomura M, Foulkes FR (2002) J Appl Electrochem 32:629
4. Qu NS, Zhu D, Chan KC, Lei WN (2003) Surf Coat Technol 168:123
5. Lin C-S, Peng K-C, Hsu P-C, Chang L, Chen C-H (2000) Mater Trans JIM 41:777
6. Barabási A-L, Stanley HE (1995) Fractal concepts in surface growth. Cambridge University Press, Cambridge
7. Saitou M, Oshikawa W, Mori M, Makabe A (2001) J Electrochem Soc 148:C780
8. Saitou M (2002) Phys Rev B 66:073416
9. Saitou M, Hamaguchi K, Oshikawa W (2003) J Electrochem Soc 150:C99
10. Gómez E, Pollina R, Vallés E (1995) J Electroanal Chem 397:111
11. Pandey PK, Sahu SN, Chandra S (1996) Handbook of semiconductor electrodeposition. Marcel Dekker Inc, New York
12. Vazquez-Arenas J, Cruz R, Mendoza-Huizar LH (2006) Electrochim Acta 52:892
13. López JM, Rodríguez MA, Cuerno R (1997) Phys Rev E 56:3993
14. Dini JW (1992) Electrodeposition, 2nd edn. Noyes Publ, New Jersey
15. Luo JK, Chu DP, Flewitt AJ, Spearing SM, Fleck NA, Milne WI (2005) J Electrochem Soc 152:C36
16. Morales J, Krijer SM, Esparza P, González S, Vázques L, Salvarezza RC, Arvia AJ (1996) Langmuir 12:1068
17. Fu T-Y, Tsong TT (2000) Surf Sci 454–456:57
18. Kollia C, Spyrellis N (1993) Surf Coat Technol 57:71